

Rings and spiral arms: are they coupled with bars?

Simón Díaz-García^{1,2}, Johan H. Knapen^{1,2}, Heikki Salo³, Martín
Herrera-Endoqui⁴, and Sergio Díaz-Suárez^{1,2}

¹Instituto de Astrofísica de Canarias, E-38205, La Laguna, Tenerife, Spain
email: simondiazgar@gmail.com

²Departamento de Astrofísica, Universidad de La Laguna, E-38205, La Laguna, Tenerife, Spain

³Astronomy Research Unit, University of Oulu, FI-90014 Finland

⁴Instituto de Astronomía, Universidad Nacional Autónoma de México, Apdo. Postal 877,
Ensenada, Baja California 22800, México

Abstract. Rings and spiral arms are distinctive features of many galaxies, and their properties are closely related to the disk dynamics. They are often associated to stellar bars, but the details of this connection are far from clear. We study the pitch angles of spiral arms and the frequency and dimensions of inner and outer rings as a function of disk parameters and the amplitude of non-axisymmetries in the S⁴G survey. The ring fraction increases with bar Fourier density amplitude: this can be interpreted as evidence for the role of bars in ring formation. The sizes of inner rings, normalised by the disk size, are positively correlated with bar strength: this can be linked to the radial displacement of the inner 4:1 ultra-harmonic resonance while the bar grows and the pattern speed decreases. The fraction of rings is larger in barred galaxies than in their non-barred counterparts, but still $\sim 1/3$ ($\sim 1/4$) of the galaxies hosting inner (outer) rings are not barred. The amplitudes of bars and spirals are correlated for all types of spirals. However, on average, the pitch angles of spiral arms are roughly the same for barred and non-barred galaxies: this questions the role of bars exciting spiral structure. We conclude that the present-day coupling of rings, spiral arms, and bars is not as robust as predicted by simulations.

Keywords. galaxies: structure - galaxies: evolution - galaxies: statistics - galaxies: spiral - galaxies: fundamental parameters - galaxies: photometry

1. Context and aims

Do galactic bars drive the formation of rings and spiral arms? Simulations predict so (e.g. Sellwood & Wilkinson 1993; Athanassoula, E. *et al.* 2013, and references therein):

- (a) most rings form from interstellar gas collected near disk resonances (e.g. Schwarz 1981; Rautiainen & Salo 2000), under the action of bar gravity torques,
- (b) bars excite spiral density waves (e.g. Sanders & Huntley 1976),
- (c) rings/spirals can be made of orbits organised in tubes (invariant manifolds) originating from close to the bar ends (e.g. Romero-Gómez *et al.* 2006).

Here, we address the coupling between bars, rings, and spirals in the *Spitzer* Survey of Stellar Structure in Galaxies (S⁴G; Sheth *et al.* 2010). We use 3.6 μm imaging for a parent sample of 1320 nearby galaxies with inclinations lower than 65° (according to Salo *et al.* 2015), of which (according to Buta *et al.* 2015) 825 are barred, 465 host inner rings, 264 host outer rings, and 391 have measurements of the pitch angle (winding angle) of the spiral arms (from Herrera-Endoqui *et al.* 2015; Díaz-García *et al.* 2019b).

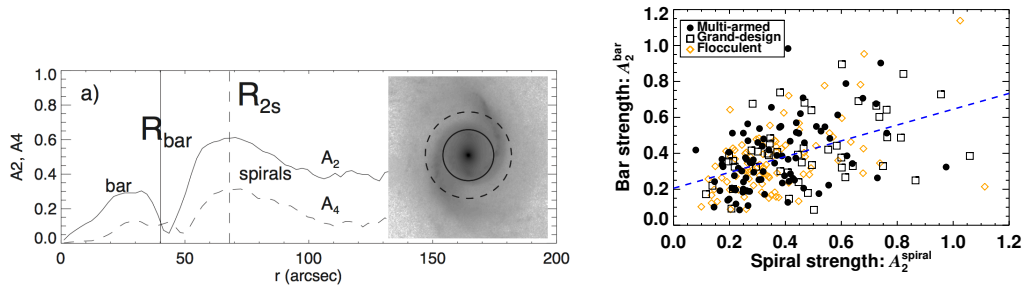


Figure 1. *Left:* Example of bar/spiral force calculation for NGC 1566 (from [Salo et al. 2010](#)). Radial profiles of the $m = 2, 4$ Fourier density amplitudes and de-projected K_S -band image (inner panel). The vertical lines indicate the bar length (solid) and the distance of maximum A_2 of the spirals (dashed) (these radii are also overlaid on the image). *Right:* Spiral strength (from [Díaz-García et al. 2019b](#)) versus bar strength (from [Díaz-García et al. 2016a](#)), measured from A_2 using $3.6 \mu\text{m}$ imaging. Different colours and symbols represent different types of spirals (see legend). The dashed blue line shows the linear fit to the cloud of points.

2. Strength of spiral arms and bars

We calculate the amplitudes of non-axisymmetries from the maximum of the $m = 2$ normalised Fourier density amplitudes (A_2) associated to the bar (A_2^{bar} , from [Díaz-García et al. 2016a](#)) and to the spiral arms (A_2^{spiral} , from [Díaz-García et al. 2019b](#)) (left panel on Fig. 1), using $3.6 \mu\text{m}$ S⁴G images.

We confirm that the strengths of bars and spirals are correlated (right panel of Fig. 1) (e.g. [Salo et al. 2010](#)). This either i) supports the role of bars driving the formation of spirals ([Sanders & Huntley 1976](#)) or ii) indicates that the disks that are prone to the formation of strong bars are also more reactive to the development of spirals of large amplitudes ([Salo et al. 2010](#); [Díaz-García et al. 2016b](#)), while the correlation does not necessarily imply causation. The latter interpretation (ii) is favoured by the observed coupling of the amplitudes of bar and arms even in flocculent spirals or when only the outermost segments of multi-armed galaxies are analysed (most likely, bars are not responsible for exciting flocculent arms or outer spiral modes) ([Díaz-García et al. 2019b](#)).

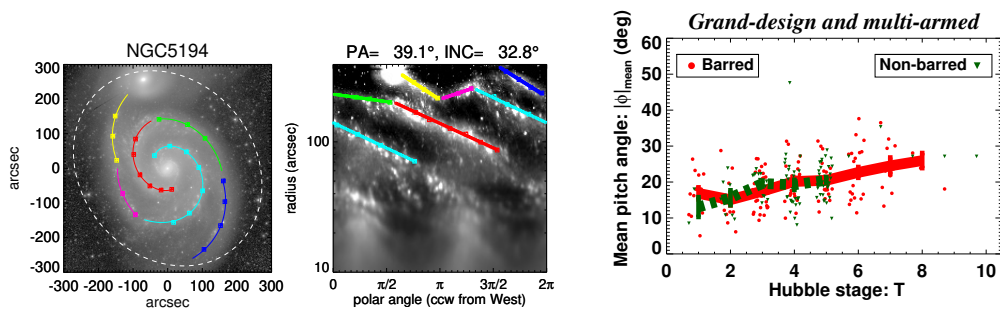


Figure 2. The $3.6 \mu\text{m}$ image of M51 in the sky plane (*left panel*) and the logarithmic polar plot de-projected to the disk plane (*central panel*). Overlaid with different colours are the fitted logarithmic spiral segments by [Herrera-Endoqui et al. \(2015\)](#). In the *right panel* we show the mean pitch angle of the galaxy as a function of the integer value of the revised numerical Hubble stage, for all the grand-design and multi-armed spirals in our sample. The running mean and standard deviation of the mean are shown for the barred (red) and non-barred (green) galaxies.

3. Pitch angle of spiral arms in barred and non-barred galaxies

Herrera-Endoqui *et al.* (2015) calculated the pitch angles of spiral arm segments using $3.6 \mu\text{m}$ S⁴G photometry. They visually marked points tracing the spiral segments and performed a linear fit in the disc plane in a polar coordinates, where logarithmic arms appear as straight lines (left and central panels of Fig. 2). In order to parameterise the global winding of the spirals, we calculate the mean of the absolute value of the pitch angle measurements of logarithmic segments ($|\phi|_{\text{mean}}$) (Díaz-García *et al.* 2019b).

For grand-design and multi-armed spirals, the global pitch angle increases with increasing Hubble type (T) (right panel of Fig. 2), as expected, but with a large scatter. Interestingly, the distribution of pitch angles for barred and non-barred galaxies is roughly the same when $1 \leq T \leq 5$: this questions the role of bars driving spiral density waves.

4. Interplay between bars and rings

Rings are more common in galaxies with stronger bars: The fraction of inner and outer rings (as identified by Buta *et al.* 2015) increases with increasing bar Fourier density amplitude (upper panels of Fig. 3): this can be interpreted as evidence for the role of bars in ring formation (Díaz-García *et al.* 2019a). However, $\sim 1/3$ ($\sim 1/4$) of the galaxies hosting inner (outer) rings are not barred (lower panels of Fig. 3), and thus i) some bars dissolve after ring formation (implausible based on simulations), or ii) other mechanisms may be responsible for ring creation (e.g. spirals or interactions).

Concurrent growth of inner rings and bars: We use measurements of sizes and axial ratios of inner and outer rings (left and central panels of Fig. 4) from Herrera-Endoqui *et al.* (2015). The sizes of inner rings are correlated with bar strength (right panel of Fig. 4): we interpret this as a consequence of the concurrent growth of bars (whose strength and length increase in time) and inner rings, as the inner 4:1 ultraharmonic

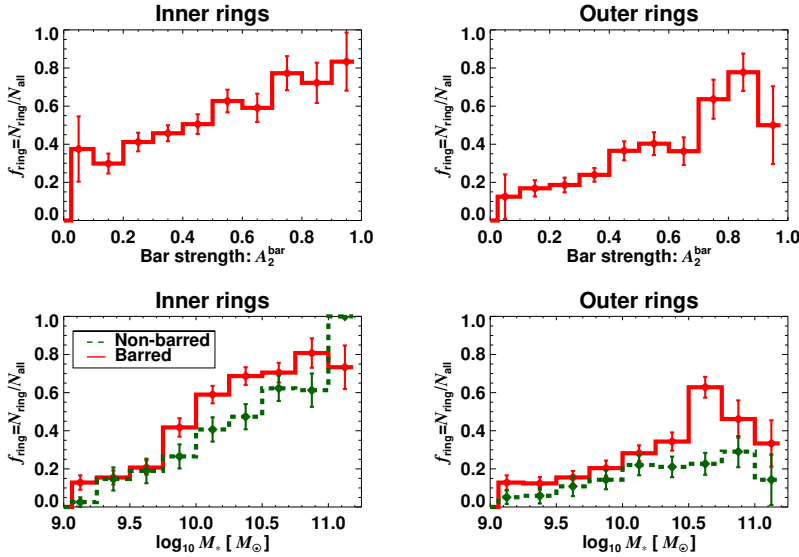


Figure 3. Fraction of inner (*left*) and outer (*right*) rings as a function of $m = 2$ bar Fourier amplitude (*upper panels*) and total stellar mass of the galaxies (*lower panels*, including non-barred galaxies). Error bars correspond to binomial counting errors. The fraction of rings increases with increasing M_* and A_2^{bar} . The fraction of inner (outer) rings in barred galaxies is 1.41 ± 0.12 (1.88 ± 0.25) times larger than in their non-barred counterparts (see also Comerón *et al.* 2014).

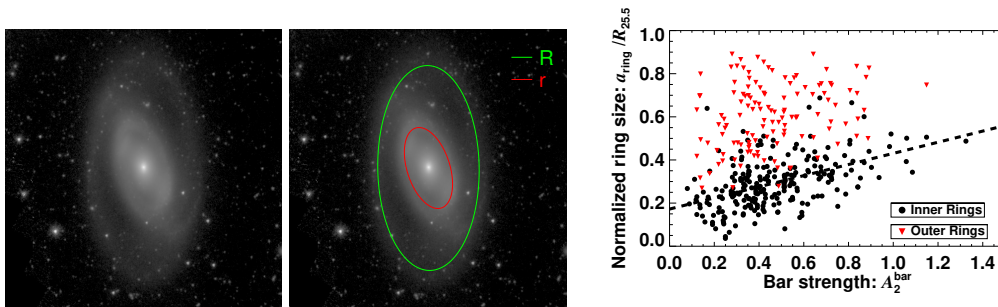


Figure 4. *Left and central panels:* Measurements of the sizes and axial ratios of the inner (red) and outer (green) rings hosted by NGC 1350 (from Herrera-Endoqui *et al.* 2015). The outline of the ridge of the rings was visually marked and fitted with an ellipse on the $3.6 \mu\text{m}$ images. *Right panel:* For a sample of non-highly inclined disk galaxies, de-projected semi-major axis of rings, normalised to $R_{25.5}$ (isophotal radii at $25.5 \text{ mag arcsec}^{-2}$ at $3.6 \mu\text{m}$, from Muñoz-Mateos *et al.* 2015), versus the $m = 2$ bar Fourier amplitude (Díaz-García *et al.* 2019a), separating inner and outer rings (see legend). The dashed line shows the linear fit to the data cloud for inner rings.

resonance moves outwards in the disc while the pattern speed decreases (Díaz-García *et al.* 2019a). Outer ring sizes do not correlate with bar strength: this is probably linked to the larger timescales required for outer ring formation from gas redistributed by bars, whose potential might have changed in time.

5. Conclusions

- Bars play a role in inner/outer ring formation. However, the coupling between bars and rings is not as strong as expected from numerical models (Díaz-García *et al.* 2019a).
- Disks that are prone to the development of strong bars are also reactive to the formation of prominent spirals. This does not imply that spirals are bar-driven. Statistically, barred and non-barred galaxies have similar pitch angles (Díaz-García *et al.* 2019b).

References

- Athanassoula, E. 2013, *Bars and secular evolution in disk galaxies: Theoretical input*, ed. J. Falcon-Barroso & J. H. Knapen, 305
- Buta, R. J., Sheth, K., Athanassoula, E., et al. 2015, *ApJS*, 217, 32
- Comerón, S., Salo, H., Laurikainen, E., et al. 2014, *A&A*, 562, A121
- Díaz-García, S., Salo, H., Laurikainen, E., & Herrera-Endoqui, M. 2016a, *A&A*, 587, A16
- Díaz-García, S., Salo, H., & Laurikainen, E. 2016b, *A&A*, 596, A84
- Díaz-García, S., Díaz-Suárez, S., Knapen, J. H., & Salo, H. 2019a, *A&A*, 625, A146
- Díaz-García, S., Salo, H., Knapen, J. H., & Herrera-Endoqui, M. 2019b, *A&A*, accepted, in press
- Herrera-Endoqui, M., Díaz-García, S., Laurikainen, E., & Salo, H. 2015, *A&A*, 582, A86
- Julian, W. H. & Toomre, A. 1966, *ApJ*, 146, 810
- Muñoz-Mateos, J. C. et al. 2015, *ApJS*, 219, 3
- Rautiainen, P. & Salo, H. 2000, *A&A*, 362, 465
- Romero-Gómez, M. et al. 2006, *A&A*, 453, 39
- Salo, H., Laurikainen, E., Buta, R., & Knapen, J. H. 2010, *ApJ*, 715, L56
- Salo, H., Laurikainen, E., Laine, J., et al. 2015, *ApJS*, 219, 4
- Sanders, R. H., & Huntley, J. M. 1976, *ApJ*, 209, 53
- Schwarz, M. P. 1981, *ApJ*, 247, 77
- Sellwood, J. A. & Wilkinson, A. 1993, *Reports on Progress in Physics*, 56, 173
- Sheth, K., Regan, M., Hinz, J. L., et al. 2010, *PASP*, 122, 1397